# RESEARCH PAPER

# Characterization of hadrucalcin, a peptide from *Hadrurus gertschi* scorpion venom with pharmacological activity on ryanodine receptors

Elisabeth F Schwartz[1,2]*, E Michelle Capes[3]*, Elia Diego-García[2], Fernando Z Zamudio[2], Oscar Fuentes[3,4], Lourival D Possani[2] and Héctor H Valdivia[3]

[1]*Department of Physiological Sciences, Institute of Biological Sciences, University of Brasilia, Brasilia, Brazil,* [2]*Department of Molecular Medicine and Bioprocesses, Instituto de Biotecnología, Universidad Nacional Autónoma de Mexico, Cuernavaca, México,* [3]*Department of Physiology, University of Wisconsin Medical School, Madison, WI, USA, and* [4]*Departamento de Ciencias Básicas, Facultad de Ciencias, Universidad del Bío-Bío, Chillán, Chile*

**Background and purpose:** Members of the calcin family, presently including imperatoxin A, maurocalcin, opicalcins and hemicalcin, are basic, 33-mer peptide activators of ryanodine receptors (RyRs), the calcium channels of the sarcoplasmic reticulum (SR) that provide the majority of calcium for muscle contraction. Here we describe hadrucalcin, a novel member of this family.

**Experimental approach:** Hadrucalcin was isolated from the venom of *Hadrurus gertschi*. Amino acid sequence and mass were determined by Edman degradation and mass spectrometry respectively. A cDNA library was constructed to generate clones for DNA sequence determination. Biological activity of native toxin was confirmed with [$^3$H]ryanodine binding, by using SR vesicles from cardiac and skeletal muscle, and with single skeletal (RyR1) and cardiac (RyR2) channels reconstituted in lipid bilayers. Hadrucalcin was applied to intact ventricular myocytes to investigate effects on calcium transients. The secondary structure of hadrucalcin was computer-modelled by using atomic coordinates from maurocalcin, a structurally similar peptide.

**Key results:** Hadrucalcin is distinguished from previously described congeners by two additional amino acids in its primary sequence and the lack of prominent amphipathicity. Hadrucalcin activated RyRs with high affinity ($EC_{50} = 37$ nmol·L$^{-1}$), induced a long-lasting subconductance state on RyR1 and RyR2, and rapidly (lag time ~2 s) penetrated ventricular cardiomyocytes, eliciting discharge of internal calcium stores and spontaneous contractions.

**Conclusions and implications:** Hadrucalcin is a cell-permeant, powerful activator of RyRs, which has translational potential for targeted delivery of drugs to RyR as novel therapeutic intervention in arrhythmogenic disease.
*British Journal of Pharmacology* (2009) **157**, 392–403; doi:10.1111/j.1476-5381.2009.00147.x; published online 22 April 2009

## Introduction

Venoms of snakes, spiders and scorpions are used for defence and predation, with the goal of immobilizing opponents or potential prey. As a result, these venoms are rich in peptide toxins that target voltage- and ligand-gated ion channels, the molecular components that trigger locomotion. In fact, toxins isolated from venomous organisms have been extensively exploited as a source of specific probes for these channels (Possani *et al.*, 1999).

In excitable cells, elevation of intracellular Ca$^{2+}$ concentration ([Ca$^{2+}$]$_i$, intracellular calcium concentration) initiates a cascade of signal transduction events that culminates in a variety of physiological processes including secretion of hormones and neurotransmitters, activation of transcription factors, egg fertilization, muscle contraction and many others

Correspondence: Héctor H Valdivia, Department of Physiology, University of Wisconsin Medical School, Madison, WI 53706, USA. E-mail: valdivia@physiology.wisc.edu
*These authors contributed equally to this study.

A novel toxin that activates ryanodine receptors
EF Schwartz *et al*
393

(Berridge, 1997). In mammals, reptiles, insects and other animal taxa, depolarization of the external membrane of cardiac and skeletal muscle cells activates voltage-dependent $Ca^{2+}$ channels (also known as dihydropyridine receptors, DHPRs), which in turn activate $Ca^{2+}$ release channels/ryanodine receptors (RyRs) of the sarcoplasmic reticulum (SR) to elevate $[Ca^{2+}]_i$ and initiate myofilament contraction (Bers, 2001). The release of $Ca^{2+}$ by RyRs is so swift ($\tau_{on} \sim 1$ ms) and massive (80–200 $\mu mol \cdot L^{-1} \cdot s^{-1}$) that an intrinsic inactivation process is safely in place to avoid flooding of cytosolic compartments with $Ca^{2+}$ and subsequent contractile paralysis (Bers, 2001). Indeed, the plant alkaloid ryanodine causes respiratory muscle paralysis and death by opening RyRs with high potency (Sutko *et al.*, 1997). It appears, therefore, that RyRs could be natural targets for disruption should a scorpion attempt to immobilize potential prey.

Imperatoxin A (IpTx$_a$), a peptide isolated from the venom of the African scorpion *Pandinus imperator*, was the first scorpion toxin with demonstrated capacity to bind to RyRs with high affinity and specificity (Valdivia *et al.*, 1992). Unlike traditional $Na^+$ and $K^+$ channel-modifying scorpion toxins, IpTx$_a$ is a highly basic, short (33-amino acid) peptide stabilized by three disulphide bridges and folding along an inhibitor cystine-knot (ICK) motif (Zamudio *et al.*, 1997; Lee *et al.*, 2004). The presence of IpTx$_a$ in scorpion venom was surprising because as a basic peptide, this ionized molecule was presumed to be incapable of penetrating cellular membranes to reach its intended target. However, the scorpion toxin maurocalcin (MCa), which was isolated based on sequence similarity to IpTx$_a$ (Faljoun *et al.*, 2000), has been elegantly shown to penetrate external membranes (Estève *et al.*, 2005). Like IpTx$_a$, MCa displays a cluster of basic residues that resembles a protein-interacting domain, confers amphipathicity and is essential for RyR recognition and cell penetration (Estève *et al.*, 2005; Boisseau *et al.*, 2006). Other scorpion peptides with high sequence similarity to IpTx$_a$ and MCa have subsequently followed, specifically, opicalcin 1 and 2 (Opi 1, Opi 2; Zhu *et al.*, 2003) and hemicalcin (HCa; Shahbazzadeh *et al.*, 2007), all 33-mer peptides containing the critical cluster of basic residues and presumably conforming to the aforementioned ICK motif. Although only MCa has so far been shown to penetrate cellular membranes, it appears likely that all members of this family, recognized now as the calcin family for their capacity to alter $Ca^{2+}$ release channels/RyRs, are capable of permeating cells to alter $Ca^{2+}$ release, but this property has yet to be confirmed.

Here we describe the purification, gene and amino acid sequences, structural modelling and functional characterization of hadrucalcin (HdCa), a novel member of the calcin family isolated from the venom of *Hadrurus gertschi*, a scorpion endemic to Guerrero, Mexico. We also show that HdCa permeates ventricular cardiomyocytes and disrupts $Ca^{2+}$ release from internal stores with surprisingly rapid kinetics (lag time ~2 s). Unique among this family of peptides, HdCa is composed of 35 amino acids and 13 spirally arranged basic residues, which in the aggregate impart a rather uniform distribution of positive charges, a reduced dipole moment and surprisingly little amphipathicity, challenging the notion that the latter is required to penetrate cellular membranes.

## Methods

### Animals
Animal care and handling conformed to the Guide for Care and Use of Laboratory Animals published by the US National Institutes of Health (NIH publication no. 85–23, revised 1996), and experimental protocols were approved by the local institutional ethical committee. Dogs, rabbits and mice, the animals used in this study, were maintained in environmentally controlled rooms with 12 h light/dark cycles and adequate food and water, where they were assessed daily for well-being by trained veterinary personnel. For experiments with mouse tissue, 3 to 5-month-old mice ($n = 34$) were injected i.p. with 0.075 mL heparin and then killed by cervical dislocation. Dog tissue used in this study was obtained from an adult male beagle (11 kg), anaesthetized with inhaled isoflurane (3–5%, applied by mask). Rabbit tissue was obtained from an adult female New Zealand White rabbit (3.5 kg), anaesthetized by i.p. injection of pentobarbital (100 mg/kg). Adequacy of anaesthesia was assessed by pedal reflex and evaluation of jaw and muscle tone before proceeding with surgery to remove the heart.

### Venom source and purification procedures
Venom from *H. gertschi* Soleglad, 1976 (Scorpiones : Caraboctonidae) was obtained by electrical stimulation of telsons (last post-abdominal segment) from scorpions captured in the State of Guerrero, Mexico. The material was extracted with water and centrifuged at $10\,000 \times g$ for 10 min. The soluble supernatant was either lyophilized or stored at –20°C, and later separated by high-performance liquid chromatography essentially as described earlier (Schwartz *et al.*, 2006). Briefly, whole venom was injected into a C18 reverse-phase semi-preparative column (Vydac, Hisperia, CA, USA) and separated by using a linear gradient from solvent A (0.12% trifluoroacetic acid, TFA, in water) to 60% solvent B (0.10% TFA in acetonitrile) run for 60 min, at a flow rate of 2 mL·min$^{-1}$. The fraction of interest from several independent runs were pooled and further purified on a C18 reverse-phase analytic column (Vydac, Hisperia, CA, USA) to obtain HdCa in homogeneous form, as shown by mass spectrometry analysis and amino acid sequencing (see Figure 1 for further details).

### Amino acid sequence determination and mass spectrometry analysis
The amino acid sequence of HdCa was obtained by automatic Edman degradation in a Beckman LF 3000 Protein Sequencer (Palo Alto, CA, USA) using the chemicals and procedures previously described for other peptides of this venom (Schwartz *et al.*, 2006). The molecular mass of HdCa was obtained by mass spectrometer analysis, using a Finnigan LCQ$^{DUO}$ (San Jose, CA, USA), also as described previously (Schwartz *et al.*, 2006).

### cDNA library construction
A cDNA library was constructed with total RNA extracted from a single telson of a *H. gertschi* scorpion. For RNA
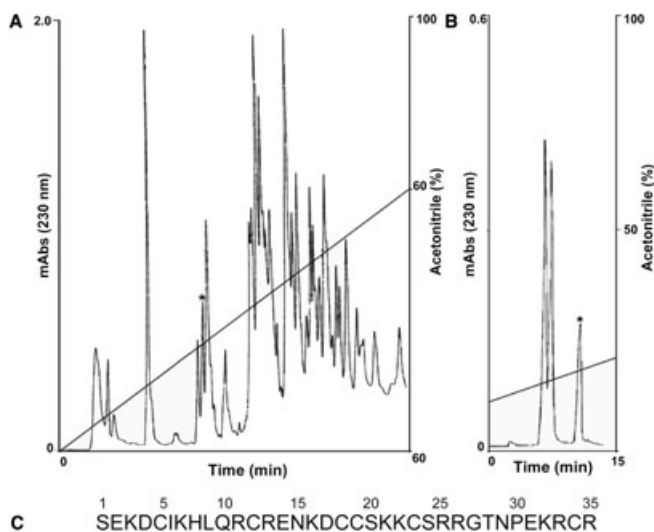
**Figure 1** Purification and characterization of hadrucalcin (HdCa). (A) 4 mg of soluble venom from *Hadrurus gertschi* was separated by high-performance liquid chromatography using a semi-preparative C18 reverse-phase column, eluted with a linear gradient from solution A to 60% solution B run for 60 min. The fraction labelled with the asterisk was re-chromatographed in a analytical C18 reverse-phase column and run from 90% solution A to 30% solution B in 30 min. (B) The component with retention time of 12.24 min (labelled with asterisk) is pure HdCa. (C) The complete amino acid sequence of HdCa was obtained by a combination of direct Edman degradation and mass spectrometry, as described in the text. The amino acid sequence has been deposited in UniProt Knowledgebase with accession number P85499.

isolation the 'Total RNA Isolation System' of Promega (Madison, WI, USA) was used. With this material a full-length cDNA phagemid library was prepared by using the SMART cDNA Library Construction Kit (Clontech Lab, Palo Alto, CA, USA). The titre of the amplified cDNA library obtained was $5.23 \times 10^{10}$ cfu·mL$^{-1}$ with 99% recombinant clones.

### Gene cloning and DNA sequencing

Based on the information obtained from direct peptide sequencing, three oligonucleotides were synthesized, Hadru5EKDC: 5′-GAR AAR GEY TGY ATH AAR CAY YTN CA-3′, HadruEKD3: 5′-CAN CKY TTY TCN GGR TTN GTN CC-3′ and HgSEKD3′: 5′-GAT TTA TCT GCA TCT CTT TTC C-3′ using a model 391 DNA Synthesizer from Applied Biosystems (Foster City, CA, USA) where R, E, Y, H and N stand for degenerate nucleotides. These oligonucleotides were used in conjunction with the pairs TripIEx2-5′ and TroIEx2-3′ from Clontech Lab (Palo Alto, CA, USA) for PCR amplification, by using material from the cDNA library. The PCR reaction was performed in 1× Taq DNA polymerase PCR buffer, 200 μmol·L$^{-1}$ dNTPs, 10 pmol both primers and 2 units of Taq DNA polymerase Recombinant (Invitrogen, Brazil) in 50 μL final volume. The PCR protocol was: one initial pre-cycle 3 min denaturation at 94°C, 5 min alignment at 42°C, 3 min elongation at 72°C. After this cycle the mixture was incubated for 50 s for denaturation at 94°C, 1 min alignment at 50°C, 1 min elongation at 72°C, repeated 32 cycles, followed by a final step at 72°C for 7 min. PCR products were purified by

using a Centricon 100 column (Amicon, Beverley, MA, USA) following the manufacturer instructions, and the PCR fragments were cloned into the pGEM plasmid (Promega, Madison, WI, USA). This vector was used to transform competent DH5-α *Escherichia coli* cells. Positive clones were sequenced from both ends by using an automatic sequencer (Model 3100, Applied Biosystems, Foster City, CA, USA). The nucleotide sequence obtained in this work was deposited in GenBank (accession number: EU496812).

### Preparation of SR vesicles and [³H]ryanodine binding assay

Heavy SR was prepared from rabbit white back and leg muscle (RyR1) and from canine ventricular tissue (RyR2) by using the procedure described by Meissner and Henderson (1987). [³H]ryanodine binding to rabbit skeletal SR and canine cardiac heavy SR was carried out as previously described (El-Hayek *et al.*, 1995; Gurrola *et al.*, 1999). Briefly, the standard incubation medium contained 0.2 mol·L$^{-1}$ KCl, 1 mmol·L$^{-1}$ Na$_2$EGTA, 10 mmol·L$^{-1}$ Na-PIPES (pH 7.2) and CaCl$_2$ to set free [Ca$^{2+}$] in the range of 10 nmol·L$^{-1}$ to 10 mmol·L$^{-1}$. Ca$^{2+}$/EGTA ratio was calculated by using the computer programme Max-Chelator (http://www.stanford.edu/~cpatton/maxc.html). [³H]ryanodine (68.4 Ci·mmol$^{-1}$, Dupont NEN, Wilmington, DE, USA) was diluted directly in the incubation medium to a final concentration of 7 nmol·L$^{-1}$. Protein concentration was in the range of 0.2–0.6 mg·mL$^{-1}$ and was determined by the Bradford method. Incubation lasted for 90 min at 36°C. Samples (0.1 mL) were always run in duplicate, filtered on Whatman GF/C glass filters (Whatman, Clifton, NJ, USA) and washed twice with 5 mL of distilled water using a Brandel M24-R cell harvester (Gaithersburg, MD, USA). Non-specific binding was determined in the presence of 10 μmol·L$^{-1}$ unlabelled ryanodine and has been subtracted from each sample.

### Single channel experiments

Two sources of RyRs were used for single channel experiments. RyR1 was from rabbit white skeletal muscle SR vesicles (obtained as described above), and RyR2 was from HEK293 cells expressing the mouse wild-type *RYR2* gene (a generous gift from Dr Wayne Chen, with methods and reagents for transfection and expression as outlined in Liu *et al.*, 2002). Recombinant wild-type RyR2 channels were purified from detergent-solubilized HEK293 cell lysates by sucrose density gradient centrifugation as originally described by Lai *et al.* (1988) with modifications by Li and Chen (2001). Recordings of single RyR channels reconstituted in lipid bilayers were made as previously described (El-Hayek *et al.*, 1995; Gurrola *et al.*, 1999). Briefly, planar lipid bilayers composed of phosphatidylethanolamine : phosphatidylserine (1:1) were painted with a glass rod across an aperture of ~200 μmol·L$^{-1}$ diameter in a Delrin cup. The *cis* chamber represented the cytosolic side, which was held at virtual ground and contained the reference electrode. The *trans* chamber corresponded to the luminal side and contained the voltage command electrode, connected to the head stage of a 200A Axopatch amplifier (Axon Instruments, Foster City, CA, USA). For RyR1 experiments, the *cis* (0.7 mL) and *trans* (0.7 mL) chambers were initially filled with 50 mmol·L$^{-1}$ caesium

A novel toxin that activates ryanodine receptors
EF Schwartz *et al*
395

methanesulphonate and 20 mmol·L$^{-1}$ MOPS, pH 7.2. After bilayer formation, capacitance was checked by using a square pulse of ±5 mV, and an asymmetric caesium methanesulphonate gradient (300 mmol·L$^{-1}$ *cis*, 50 mmol·L$^{-1}$ *trans*) was established. Rabbit skeletal SR vesicles (20–50 μg) were added to the *cis* chamber. Channel fusion recordings were made in symmetrical 300 mmol·L$^{-1}$ caesium methanesulphonate solution after dissipation of the 50 mmol·L$^{-1}$ gradient in the *trans* chamber. Experiments with RyR2 differed only in the amount of protein added (~1 μg purified mouse RyR2), and the composition of the solution: RyR2 channel fusion recordings were made in symmetrical 250 mmol·L$^{-1}$ KCl + 25 mmol·L$^{-1}$ HEPES solution. Data were collected at steady voltages (–40 and +40 mV). Single channel recordings were filtered with an 8-pole low-pass Bessel filter set at 1.5 kHz and digitized at a rate of 4 kHz by using a Digidata 1200 AD/DA interface. Data acquisition and analysis were performed with Axon Instruments (Burlingame, CA, USA) hardware and software (pClamp 8) and graphed by using Origin 7.5 (Microcal Inc., Northampton, MA, USA).

*Ventricular myocyte isolation and Ca$^{2+}$ imaging of ventricular myocytes*

Mouse ventricular myocytes were isolated by collagenase digestion of perfused mouse hearts by using the method of Mitra and Morad (1985) with slight modifications. Mice were killed as described above before removal and cannulation of the heart. Cells were suspended in Tyrode solution (in mmol·L$^{-1}$): 130 NaCl, 1 CaCl$_2$, 5.4 KCl, 0.4 NaH$_2$PO$_4$, 0.5 MgCl$_2$, 22 glucose, 0.01 μg·mL$^{-1}$ insulin, 25 HEPES (pH 7.4 with NaOH) and kept at room temperature until used, normally within 6 h. Changes in cytosolic [Ca$^{2+}$] were tracked by using the Ca$^{2+}$ fluorescent dye Fluo-3 AM. Fluo-3 AM was added to ventricular myocytes in Tyrode solution (final concentration 10 μmol·L$^{-1}$) and incubated at room temperature for 30 min. The cells were washed and resuspended in normal Tyrode solution supplemented with 1.8 mmol·L$^{-1}$ CaCl$_2$. Fluorescence changes were monitored with a Zeiss confocal microscope in line-scan mode. Fluo-3 was excited with an Argon laser at 488 nm, and emissions were collected at 500–570 nm. Cells were perfused with normal Tyrode solution and pre-paced by field stimulation at 1 Hz for a period of 20 s to allow internal Ca$^{2+}$ stores to reach steady state. After recording normal [Ca$^{2+}$]$_i$ transients, perfusion was rapidly changed to the same Tyrode solution but supplemented with 300 nmol·L$^{-1}$ HdCa. Rapid exchange of solutions onto the surface of cardiomyocytes was achieved with a piezoelectric-controlled three-barrelled mini-perfusion system (model SF-77b Perfusion Fast-Step, Warner Instruments, Hamden, CT, USA). The lag time to switch solutions is ~50 ms, according to manufacturers' measurements. To estimate the Ca$^{2+}$ load of the SR, we performed a rapid application of 10 mmol·L$^{-1}$ caffeine to elicit discharge of RyR-gated Ca$^{2+}$ stores.

*Molecular modelling*

A set of 14 solutions was obtained by using the HdCa sequence and BLAST version 2.2.13 (http://blast.ncbi.nlm.nih.gov/BLAST.cgi) to search for similar sequences in the PDB (http://www.rcsb.org/pdb/home/home.do). Two structures presented similarities of 78% and 68%, corresponding to RyR-activating scorpion peptides, MCa and IpTx$_a$ respectively. The structure of HdCa was built based on the structure of MCa, PDB code 1C6W, using Sybyl 7.1 (Tripos Inc., St. Louis, MO, USA). The molecular coordinates are included as a data supplement in the online version of this article (see Supporting Information). The final model had its stereochemistry checked by the programme PROCHECK v.3.5.4 (ftp.biochem.ucl.ac.uk) and was compared with the template structure (MCa) by using the programme Sting (available at http://www.cbi.cnptia.embrapa.br). Solvent accessible polar surface areas were calculated by using the molecular visualization programme PyMOL (DeLano Scientific, LLC, San Carlos, CA, USA).

*Statistics*

Statistical analyses were performed by using either the computer software programme Origin (v. 7.5, Microcal Inc.) or SigmaStat computer software (version 3.0, Rockware Inc., Golden, CO, USA). Data are presented as the mean ± SEM. Data were compared using a Student's *t*-test or a one-way ANOVA (with secondary comparisons made with a Student-Newman-Keuls test). Differences of $P < 0.05$ between sample means were considered significant unless otherwise stated.

*Materials*

[$^3$H]ryanodine was purchased from Dupont NEN (Wilmington, DE, USA). Phosphatidylethanolamine and phosphatidylserine were obtained from Avanti Polar Lipids, Inc. (Alabaster, AL, USA). Type II collagenase was acquired from Worthington Biochemical (Freehold, NJ, USA). Heparin was obtained from Wedgewood Pharmacy (Swedesboro, NJ, USA). Fluo-3 was purchased from Invitrogen (Carlsbad, CA, USA). All other chemicals were purchased from Sigma-Aldrich, Inc. (St. Louis, MO, USA). Indicator dye was first dissolved in dimethyl sulphoxide, and then diluted further in buffer solution.

# Results

*Isolation and primary structure determination of HdCa*

Initial fractionation of soluble venom from *H. gertschi* by high-performance liquid chromatography separated more than 60 different components (Schwartz *et al.*, 2006). The fraction eluting at 24.54 min was further purified in an analytical C18 reverse-phase column, yielding the component of interest (Figure 1A, peak labelled with asterisk). Mass spectrometry analysis of this peak revealed a single peptide with 4190.5 atomic mass units (a.m.u.). Amino acid sequence of the reduced and alkylated peptide yielded a single sequence up to residue 34. The last residue, Arg$^{35}$, was tentatively assigned based on the molecular mass. Because the sum of the masses of the first 34 amino acids was 4034.66 (M+H)$^+$, only arginine (a.m. = 156.19) could fit the experimental atomic mass of the native peptide. Thus, the theoretical average mass of the amino acid sequence shown in Figure 1C is 4190.85

| 1 | ATG AAG ACG AGT AGT CTC ACT ATC ATC TTT ATT GCG GTC ATT ATT | 45 |
| 1 | *M K T S S L T I I F I A V I I* | 15 |
| | | |
| 46 | ACA ATT ATC TGC TTG AAT ATT CAT GAT ATA GAG GCA AGA GAG ATT | 90 |
| 16 | *T I I C L N I H D I E A* <u>R E I</u> | 30 |
| | | |
| 91 | GAA TTT AAT GCT GGA AGA GTG GTA CGT AGT GAA AAG GAC TGC ATT | 135 |
| 31 | <u>E F N A G R V V R S E K D C I</u> | 45 |
| | | |
| 136 | AAA CAC CTT CAG CGA TGC CGT GAG AAC AAG GAT TGC TGC AGT AAG | 180 |
| 46 | **K H L Q R C R E N K D C C S K** | 60 |
| | | |
| 181 | AAA TGT TCA AGG AGA GGG ACA AAC CCG GAA AAG AGA TGC AGA TAA | 225 |
| 61 | **K C S R R G T N P E K R C R** stop | 75 |

**Figure 2** Complete gene and amino acid sequence of hadrucalcin. The deduced amino acid sequence of hadrucalcin and its corresponding nucleotide sequence above. The first 28 amino acids are assumed to correspond to the signal peptide (italics) and the remainder 11 amino acids to a pro-sequence (underlined).

$(M+H)^+$, which corresponds well with the experimental value of the native peptide. We have termed this peptide HdCa, from the genus of the scorpion and its great similarity to other peptide members of the calcin family (see below). HdCa, like all members of the calcin family, is a highly basic peptide. Its theoretical isoelectric point (pI) is 9.50.

### Gene cloning and DNA sequencing

Degenerate oligonucleotides synthesized according to the amino acid sequence of HdCa were used to screen a cDNA library from the venom glands of *H. gertschi* scorpion. This procedure allowed the identification of a long DNA segment corresponding to the majority of the HdCa gene. The full DNA sequence was obtained by 5′-RACE and 3′-RACE using the nucleotides indicated in *Methods*. Figure 2 shows that the gene encoding for HdCa contains a long putative signal peptide with a pro-sequence that spans 39 amino acids, from which the first 28 are assumed to correspond to the signal peptide and the remainder 11 amino acids to a pro-sequence (italicized and underlined respectively). The segment of the gene corresponding to the mature peptide yielded an amino acid sequence identical to the 34 amino acids directly identified by Edman degradation and the arginine inferred from molecular mass. We thus confirmed the accuracy of the amino acid sequence given in Figure 1C.

### Amino acid sequence of peptides of the calcin family

Figure 3 shows the amino acid sequence of peptides of the calcin family. HdCa, which is the subject of this communication, is the only peptide for which both the gene and the peptide sequence have been obtained. Opi 1 and 2 show 81% and 78% sequence identity with HdCa, respectively, but both peptides have yet to be isolated and tested for effects on RyRs. MCa has 78% identity with HdCa and has been functionally characterized (Mosbah *et al.*, 2000). HCa bears 76% sequence identity to HdCa and was recently isolated and demonstrated to affect RyR activity (Shahbazzadeh *et al.*, 2007). IpTx$_a$ is 68% identical to HdCa and has been extensively characterized, both structurally (Zamudio *et al.*, 1997; Lee *et al.*, 2004) and functionally (Valdivia *et al.*, 1992; El-Hayek *et al.*, 1995; Trypathy *et al.*, 1998; Gurrola *et al.*, 1999).

### Molecular modelling of HdCa

As expected from the considerable degree of sequence similarity to MCa and IpTx$_a$, the only two peptides from this family whose three-dimensional conformations have been obtained (Mosbah *et al.*, 2000; Lee *et al.*, 2004), HdCa is predicted to fold along an ICK motif, although without the prominent β-sheets present in both MCa and IpTx$_a$ (Figure 3B). As a result, the globular structure of HdCa appears slightly more compact than the two previously described toxins (molecular solvent accessible polar surface area approximately 2808, 2721 and 2619 Å² for MCa, IpTx$_a$ and HdCa respectively). The primary sequence of HdCa has positively charged lysines distributed more N-terminally than any other known peptide member of the calcin family. The electrostatic properties of these toxins is likely to affect membrane translocation and RyR docking and activation, and the differences in sequence and globular structure prompted us to compare the orientation of the positively charged, basic residues on the globular structure of HdCa with those in IpTx$_a$ and MCa (Figure 3C). These residues are oriented mostly on one face of IpTx$_a$ and MCa, imparting a high degree of amphipathicity and an important dipole moment, calculated as 189 and 176 respectively. In contrast, the basic residues of HdCa are spirally oriented, which effectively reduces the dipole moment of the molecule to a calculated value of 56 and is likely to change the electrostatic environment within the binding site. Furthermore, this appears to challenge the notion that amphipathicity is required for membrane translocation capability in this family of toxins (Estève *et al.*, 2005; Mabrouk *et al.*, 2007).

### HdCa stimulates [³H]ryanodine binding to RyR1; synergistic effect of caffeine

IpTx$_a$ and MCa, the two most studied members of the calcin family, dramatically enhance the binding of [³H]ryanodine to RyR1, the skeletal isoform of RyRs (Valdivia *et al.*, 1992; Zamudio *et al.*, 1997; Faljoun *et al.*, 2000; Lee *et al.*, 2004; Estève *et al.*, 2005; Boisseau *et al.*, 2006). We thus tested the effect of HdCa, a peptide structurally similar to IpTx$_a$ and MCa, expecting similar results. Figure 4A shows that HdCa is indeed capable of enhancing [³H]ryanodine binding to skeletal SR vesicles, with half-maximal effective concentration $(ED_{50}) = 37 \pm 8$ nmol·L⁻¹ and a potency (% of stimulation) = $402 \pm 62\%$. The $ED_{50}$ value is higher than that of MCa (~25 nmol·L⁻¹) (Faljoun *et al.*, 2000; Mabrouk *et al.*, 2007), and IpTx$_a$ (~10 nmol·L⁻¹) (Valdivia *et al.*, 1992; Gurrola *et al.*, 1999), but lower than that of HCa (71 nmol·L⁻¹) (Shahbazzadeh *et al.*, 2007).

We also tested whether caffeine, a classical activator of RyRs (Rousseau *et al.*, 1988), shares similar or interacting binding sites with HdCa. Figure 4B shows the effect of caffeine alone and in combination with HdCa. At *p*Ca 7, binding was 0.058 ± 0.008 pmol·mg⁻¹ in the absence of HdCa and caffeine and increased to 0.151 ± 0.027 pmol·mg⁻¹ in the presence of 30 mmol·L⁻¹ caffeine, that is, an increase of 260 ± 46% (mean ± SE *n* = 3). This effect was rather modest, but is consistent with previous determinations carried out at low [Ca²⁺] (El-Hayek *et al.*, 1995; Zamudio *et al.*, 1997). In the presence of 50 nmol·L⁻¹ HdCa, binding was 0.92 ± 0.12 pmol·mg⁻¹ in the absence of caffeine and increased to 0.352 ± 0.04 pmol·mg⁻¹ in the presence of 30 mmol·L⁻¹ caffeine, that is, a gain of 2.60 ± 0.03 pmol·mg⁻¹, or an increment of 603 ± 72%. Thus, the binding increment induced by the combined
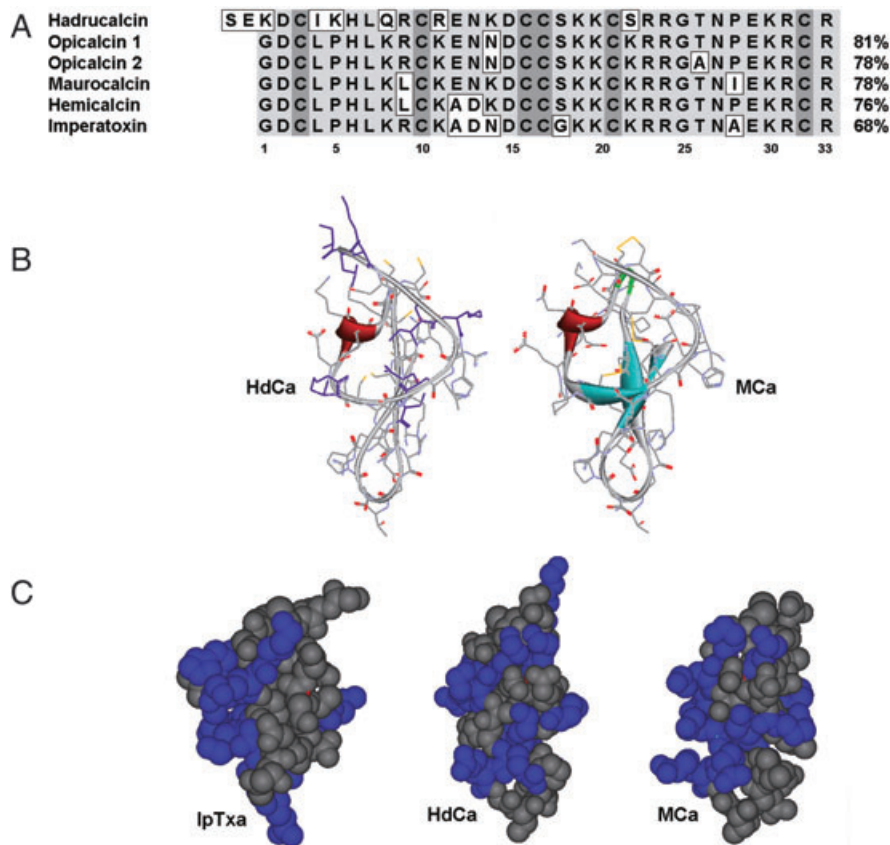
A novel toxin that activates ryanodine receptors
EF Schwartz *et al*
397

**Figure 3** Sequence homology of the calcin family and molecular models of hadrucalcin (HdCa). (A) Sequence alignment of HdCa with other scorpion peptides that activate ryanodine receptors. Imperatoxin A (IpTx$_a$) from *Pandinus imperator* (Zamudio *et al.*, 1997) maurocalcin (MCa) from *Scorpio maurus* (Faljoun *et al.*, 2000), opicalcin 1 and 2 are sequences predicted from *Opistophthalmus carinatus* (Zhu *et al.*, 2003). (B) Homology model of HdCa compared with MCa. The model was based on the atomic coordinates of MCa, with which it has the highest degree of sequence identity, using the programme Sybyl (Tripos, Inc.). (C) Orientation of basic residues (blue) on the globular structures of IpTx$_a$ (left), HdCa (middle) and MCa (right).
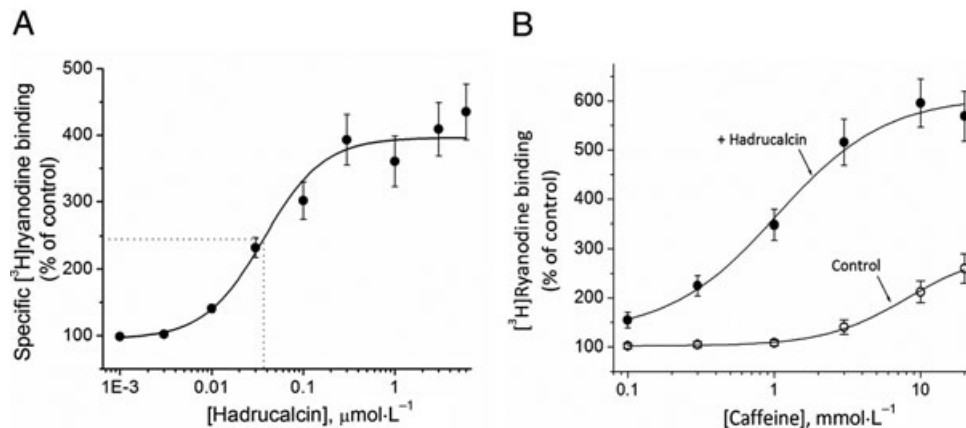


**Figure 4** Activation of [³H]ryanodine binding by HdCa (hadrucalcin) and synergistic effect with caffeine. (A) Heavy sarcoplasmic reticulum vesicles from rabbit skeletal muscle were incubated with 7 nmol·L$^{-1}$ [³H]ryanodine in the absence (control) and the presence of indicated concentrations of HdCa. Binding conditions were as specified in *Methods*. The ED$_{50}$ was $37 \pm 8$ nmol·L$^{-1}$ (mean $\pm$ SE, $n = 3$) and was determined with the formula $B = (B_{max})/[1 + (ED_{50}/[HdCa])^{nH}]$, where $B$ is specific binding of [³H]ryanodine, $B_{max}$ is the maximum binding stimulated by HdCa, and $nH$ is the Hill coefficient (1.3).

addition of caffeine and HdCa was substantially larger than the sum of the individual stimulation induced by caffeine and HdCa. This synergistic effect suggests a cooperative interaction between the HdCa and the caffeine binding sites.

*Ca²⁺ modulates the effect of HdCa on RyRs*

Ca²⁺ is critical for the binding of [³H]ryanodine to RyRs and for detection of the HdCa effect. Figure 5A shows the Ca²⁺ dependence of [³H]ryanodine binding to skeletal RyRs (RyR1)
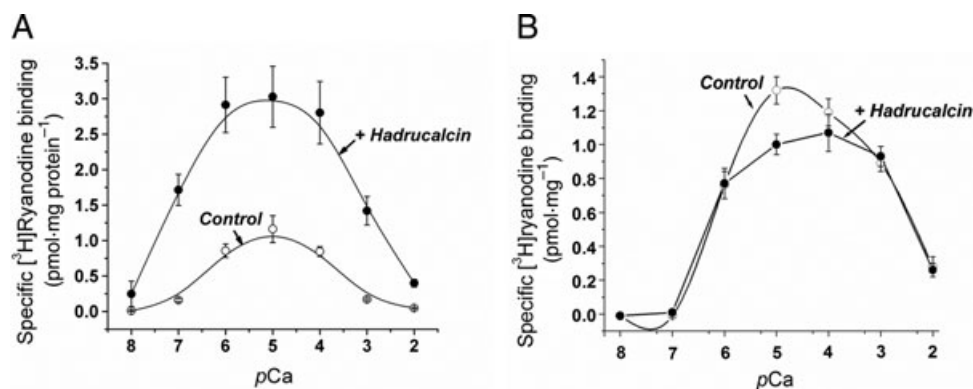
**Figure 5** Effect of HdCa (hadrucalcin) on the $Ca^{2+}$ dependence of [$^3$H]ryanodine binding to skeletal and cardiac ryanodine receptors. The $Ca^{2+}$ dependence of [$^3$H]ryanodine binding to sarcoplasmic reticulum vesicles of rabbit skeletal muscle (A) or dog cardiac sarcoplasmic reticulum (B) in the absence (open circles) and the presence (filled circles) of 100 nmol·$L^{-1}$ HdCa. Binding conditions were as described in *Methods*. Smooth lines are Bezzier fittings to the data points. Data in both panels represents the mean ± SE for *n* = 4 (A) and 3 (B) determinations.

and the effect of HdCa. Specific binding in the absence of HdCa (control, open circles) had a threshold for detection at ~100 nmol·$L^{-1}$ (*p*Ca 7) and was maximal at 10 µmol·$L^{-1}$ [$Ca^{2+}$]. Higher [$Ca^{2+}$] decreased binding. This dual effect of $Ca^{2+}$ gave rise to the well-known bell-shaped curve that is similar to the $Ca^{2+}$ dependence of open probability for skeletal RyRs (reviewed in Fill and Copello, 2002). The $ED_{50}$ for the activation of [$^3$H]ryanodine binding by $Ca^{2+}$ (ascending limb of the curve) was 0.7 µmol·$L^{-1}$, while that for the inhibition was 310 µmol·$L^{-1}$. In the presence of 100 nmol·$L^{-1}$ HdCa, the binding curve also had a bell shape but was dramatically augmented in absolute values. The augmentation of [$^3$H]ryanodine binding produced by HdCa increased with [$Ca^{2+}$]. At *p*Ca 8, 7 and 6, the net HdCa-stimulated binding (+HdCa-control) was 0.25 ± 0.04, 1.63 ± 0.21 and 2.01 ± 0.36 pmol·$mg^{-1}$ (mean ± SE *n* = 4). Furthermore, the threshold for activation was shifted by HdCa to *p*Ca 8 and the optimal binding to *p*Ca 5.5. This resulted in a shift of the ascending limb of the curve towards lower [$Ca^{2+}$], with a midpoint = 0.1 µmol·$L^{-1}$. On the other hand, the midpoint for the descending limb of the curve remained almost unchanged (420 µmol·$L^{-1}$). These results suggest that HdCa, like caffeine, partly exerts its stimulatory effect by sensitizing RyRs to $Ca^{2+}$, but unlike caffeine, stimulation may be detected in both limbs of the bell-shaped curve.

Hadrucalcin exerted a radically different effect on the binding of [$^3$H]ryanodine to cardiac RyRs (RyR2, Figure 5B). HdCa did not modify the threshold for detection of binding (*p*Ca 7), nor did it increase the ascending limb of the curve (104% of control at *p*Ca 6), but it actually *decreased* binding at *p*Ca values of 5 and 4 (76% and 90% of control respectively). The overall effect of HdCa on RyR2 thus appears more erratic, but the fact that the binding is specifically modified by the toxin strongly suggests that RyR2 is also a target of HdCa.

*Effect of HdCa on single RyR channels*
To further investigate the functional properties of HdCa, we reconstituted RyRs in planar lipid bilayers and determined the effect of HdCa on single channel gating. Figure 6 displays recordings of RyR1 in the absence and presence of HdCa.

Channels were activated by optimal levels of $Ca^{2+}$ (*p*Ca 5), which induced substantial levels of activity ($P_o$ = 0.76 ± 0.12, *n* = 4) and a small proportion of close events (Figure 6, upper panel). The unitary conductance of the control channel corresponded to ~700 pS, which is within the expected range for the recording solutions we used (Fill and Copello, 2002). In the absence of HdCa, current amplitude histograms representing 2 min of recording showed a symmetric peak centred at 0 pA (closed events), and a bigger peak at 28 pA (open events) (Figure 6, upper panel). Addition of 30 nmol·$L^{-1}$ HdCa induced a small increase in the duration of open events, but the most conspicuous effect was the appearance of a long-lived subconducting state measuring ~10 pA (250 pS), which corresponded to 35% of the full-conductance openings. This subconductance state is smaller than that induced by MCa (~50% of full conductance) (Faljoun *et al.*, 2000) but close to that induced by IpTx$_a$ (~25–30%) (Trypathy *et al.*, 1998) and HCa (38%) (Shahbazzadeh *et al.*, 2007) on RyR1.

Essentially similar results were obtained by addition of HdCa to RyR2 channels (Figure 7). Although HdCa increased overall $P_o$ (0.58 and 0.88 before and after HdCa), the main effect of the peptide was also the induction of a long-lasting subconductance state (Figure 7, lower traces and associated histogram). Of note, this substate represented ~50% of the full conductance level (see further discussion below). A subconductance state representing 25% of full conductance is apparent in the control traces. This is likely to represent an endogenous substate (an inherent property of RyRs) as it persisted in the presence of HdCa (see bottom panel), had lower amplitude and shorter duration than the HdCa-induced substate (compare current histograms before and after HdCa) and was impervious to further toxin addition (data not shown). In light of these results, we are confident that the substate recorded with HdCa in the medium truly represents the effect of the toxin. Thus, although HdCa effects on [$^3$H]ryanodine binding to each RyR isoform appears different (Figure 5), the peptide modifies single RyR1 and RyR2 channels in a similar fashion, in both cases increasing ion flow per unit time through the induction of a long-lasting subconductance state, an effect that is likely to induce $Ca^{2+}$ release from intracellular stores.
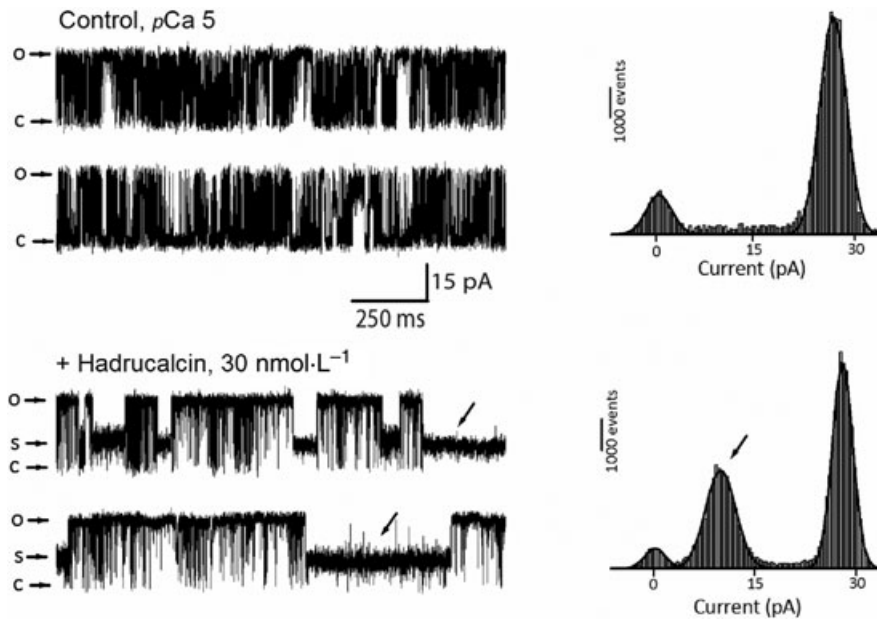
**Figure 6** Functional effect of HdCa (hadrucalcin) on single RyR1 (ryanodine receptor, skeletal isoform) activity. Heavy sarcoplasmic reticulum vesicles from skeletal muscle were fused to lipid bilayers as described in *Methods*, and the activity of single RyRs was elicited by adding 10 µmol·L$^{-1}$ Ca$^{2+}$ to the *cis* (cytosolic) side of the channel. Upper panel: left, activity of a single RyR in the absence of HdCa (control) and its corresponding current histogram (right). The closed state of the channel corresponds to 0 pA. Bottom panel: the same channel immediately after perfusion of a 2 µL solution containing HdCa (30 nmol·L$^{-1}$ final) into the *cis* side of the channel. The current histogram shows a prominent peak centred at 10 pA, which corresponds to the amplitude of the subconductance state induced by HdCa (arrows). Holding potential was 30 mV for all recordings, and openings are represented by upward deflections of the baseline current. Experiment is representative of four independent experiments.
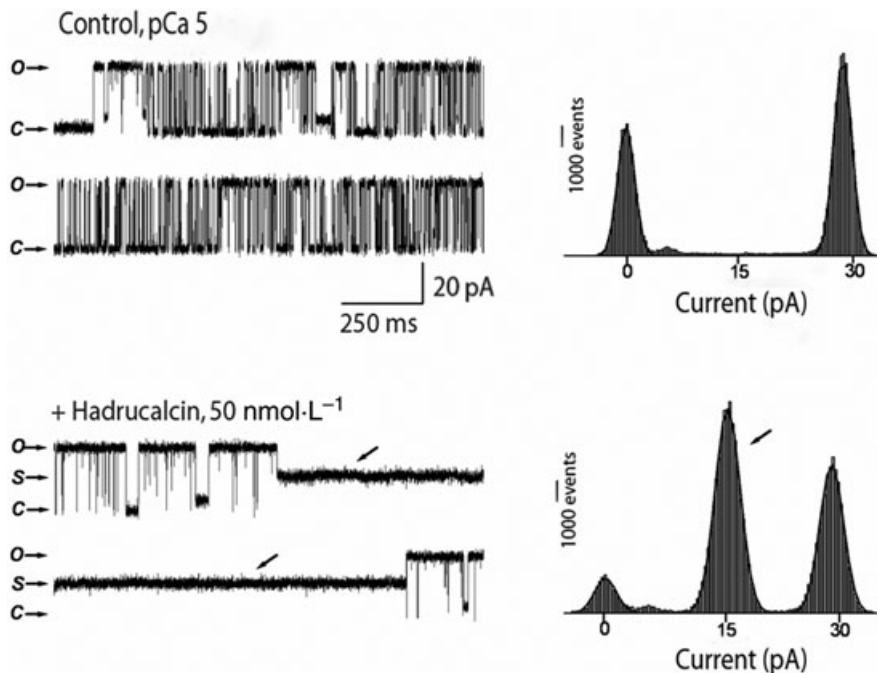


**Figure 7** Functional effect of HdCa (hadrucalcin) on single RyR2 (ryanodine receptor, cardiac isoform) activity. Purified mouse cardiac RyRs (RyR2) were fused to lipid bilayers as described in *Methods*, and the activity of single channels was elicited with a nominally free Ca solution (~5 µmol·L$^{-1}$ contaminant Ca$^{2+}$) in the *cis* (cytosolic) side of the channel. Upper panel: left, activity of a single RyR2 in the absence of HdCa (control) and its corresponding current histogram (right). The closed state of the channel corresponds to 0 pA. Bottom panel: the same channel immediately after addition of a 3.5 µL solution containing HdCa (50 nmol·L$^{-1}$ final) into the *cis* side of the channel. The current histogram shows a prominent peak centred at 10 pA, which corresponds to the amplitude of the subconductance state induced by HdCa (arrows). Holding potential was 30 mV for all recordings, and openings are represented by upward deflections of the baseline current. Experiment is representative of four independent experiments.
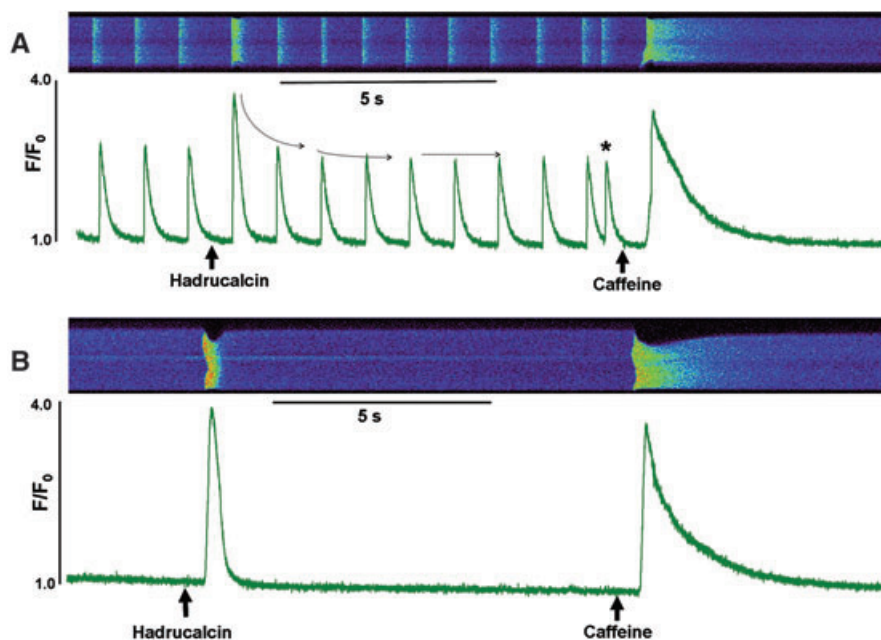
**Figure 8** Functional effect of HdCa (hadrucalcin) on global $Ca^{2+}$ handling in intact cardiomyocytes. Confocal line-scan images are aligned with $Ca^{2+}$ transients expressed as a ratio of $F/F_0$, where $F$ is fluorescence measured on a 0 to 256 arbitrary unit scale, and $F_0$ is the background fluorescence. (A) Effect of HdCa on field-stimulated single ventricular cells. The first three transients were recorded in the absence of HdCa, then the cell was rapidly perfused (indicated by the arrow) with Tyrode solution supplemented with 300 $nmol \cdot L^{-1}$ HdCa. Perfusion continued until a new solution containing 10 $mmol \cdot L^{-1}$ caffeine was added (caffeine arrow). (B) The same protocol was used, except that cells were quiescent (not electrically stimulated). Figures are representative of experiments with $n = 27$ (A) and $n = 7$ (B).

*HdCa effects on $Ca^{2+}$ handling in intact ventricular myocytes*

The selective targeting and high affinity of HdCa for RyRs, an intracellular channel raises questions about the penetration of the hydrophobic cellular membrane by a positively charged peptide in order to reach an intracellular target. We thus investigated the effect of HdCa on the intracellular $Ca^{2+}$ transients of intact ventricular myocytes. Isolated cells were loaded with the $Ca^{2+}$ indicator Fluo-3 AM, paced by field stimulation at 1 Hz for a period of 20 s to allow internal $Ca^{2+}$ stores to reach steady state, and then line-scanned with a confocal microscope to record the amplitude and kinetics of intracellular $Ca^{2+}$ ($[Ca^{2+}]_i$) transients before and after perfusion of HdCa. Figure 8A shows representative traces from such an experiment. Rapid perfusion of 300 $nmol \cdot L^{-1}$ HdCa (marked by the arrow) brought about surprisingly fast (lag time ~2 s) modifications to the $[Ca^{2+}]_i$ transients and associated contractions, first causing a robust increase in their amplitude and duration, then a gradual return to the pre-toxin steady-state level. Spontaneous $Ca^{2+}$ release events were also occasionally observed (asterisk), suggesting instability of the $Ca^{2+}$ release system in the presence of HdCa. A rapid switch to a caffeine-containing solution (10 $mmol \cdot L^{-1}$) evoked the expected massive release of $Ca^{2+}$ from the SR. In a second set of experiments (Figure 8B), we applied HdCa to quiescent (non-stimulated) cardiomyocytes to test its ability to elicit $Ca^{2+}$ release in the absence of action potential-generated sarcolemmal $Ca^{2+}$ entry. HdCa elicited short-lived $Ca^{2+}$ release that was, nonetheless, of similar amplitude to that evoked by caffeine, suggesting full activation of $Ca^{2+}$ release sites. In both sets of experiments, the integrity of the external membrane was confirmed by the ability of the cell to maintain low $[Ca^{2+}]_i$ in the presence of Ca-containing external solutions, and its responsiveness to field stimulation. Thus, HdCa appears capable of rapidly permeating the external membrane of cardiomyocytes to reach its intracellular target and evoke irregular $Ca^{2+}$ release.

## Discussion and conclusions

In this study, we have isolated and characterized a novel scorpion peptide, HdCa, which substantially expands our understanding of the structural components of the calcin family that potently activates RyRs. HdCa enhances the binding of [³H]ryanodine to RyR1 with high affinity (37 $nmol \cdot L^{-1}$, Figure 4A) and has a synergistic effect with caffeine (Figure 4B), suggesting cooperativity between the respective binding sites. The toxin activates skeletal RyR (RyR1) across a broad range of $[Ca^{2+}]$, as suggested by the [³H]ryanodine binding experiments (Figure 5A), and although it produces erratic effects on cardiac RyR (RyR2) using the same binding assay, single channel experiments (Figures 6 & 7) reveal that the toxin is equally effective in binding to the two RyR isoforms. HdCa induces the appearance of a subconductance state in both RyR isoforms that increases ion flow per unit time (Figures 6 & 7) and penetrates the cellular membrane of ventricular myocytes to cause irregular (Figure 8A) or spontaneous (Figure 8B) $Ca^{2+}$ release with extraordinarily fast kinetics (lag time ~2 s). All these characteristics are sure to contribute to the lethality or immobilization that follows a scorpion's sting; they simultaneously intensify our sense of wonderment about the inventiveness of this creature's methods of predation.

A novel toxin that activates ryanodine receptors
EF Schwartz *et al*
401

*Structural features of HdCa*

Unlike the 33-mer peptide members of the calcin family that includes IpTx$_a$, MCa, Opi 1 and 2 and HCa, only HdCa is composed of 35 amino acids and 13 (instead of 12) basic residues (Figure 3A). The presence of additional basic residues and their reshuffling in the linear sequence is probably more remarkable than the extra length of the peptide, for several reasons. First, studies with monosubstituted analogues of IpTx$_a$ (Lee *et al.*, 2004) and MCa (Mabrouk *et al.*, 2007), have defined Lys[22], Arg[23] and Arg[24] in these peptides as 'essential' or 'highly important' residues, respectively, for interaction with RyR1. This subdomain, therefore, appears to be indispensable for maintaining high affinity and perhaps specificity towards RyRs. HdCa retains the Arg-Arg pair in the equivalent subdomain (Arg[25] and Arg[26]), but it substitutes the positively charged Lys[22] with the hydroxylated Ser[24] (Figure 3A), yet it retains a high-affinity interaction with RyR1. This seems counterintuitive based on the precedent that removal of a single basic residue within this domain dramatically decreases the affinity of calcins (Gurrola *et al.*, 1999; Lee *et al.*, 2004; Estève *et al.*, 2005), but is still in agreement with the notion that these peptides, albeit small, bear *multiple* domains that contribute substantially towards their interaction with RyR1 (Lee *et al.*, 2004; Estève *et al.*, 2005). In good agreement with this notion is the fact that Lys[8], another basic residue deemed important for the interaction of IpTx$_a$ (Lee *et al.*, 2004) or MCa (Estève *et al.*, 2005) with RyR1, is also missing in HdCa (Asn[10] appears in its place). Second, some of the basic residues that HdCa does *not* have in domains previously deemed important for interaction with RyR1 are in fact in excess in other domains of the peptide. Most notably, the first segment of HdCa up to Arg[13] is populated with five basic residues representing 38.5% of total, instead of three basic residues, or 23% of total, for the other calcin members. This characteristic, unique to HdCa, substantially changes the amphipathicity of the molecule and imparts a different dipole moment to this peptide (see below). Indeed, this 13-residue region of HdCa is the most diverse among members of the calcin family, being identical to the other sequences in only five residues (38%), and even less identical (23%) if we subtract from the comparison the obligatory disulphide-forming residues Cys[3] and Cys[10]. As all calcin members so far tested display grossly similar affinity towards RyR1, this suggests that this region is perhaps of the lowest importance towards recognizing RyRs. By contrast, the last five residues of these peptides are completely conserved, and the last eleven residues differ by no more than one residue (>90% identity), clearly elevating this region to a privileged position in defining the decisive elements of calcin structure.

The structural considerations above apply remarkably well when the *linear* sequence of calcins is analysed; however, all of these peptides are highly stable, *globular* structures and residues that appear far away in the linear sequence come together and interact in the cyclotide. The ICK motif, first recognized by Pallaghy *et al.* (1994) and Narasimhan *et al.* (1994), is composed of an anti-parallel, triple-stranded β-sheet stabilized by a cystine-knot. Our modelling studies indicate that the molecular architecture of HdCa is composed of an ICK fold constrained by three intramolecular disulphide bonds. This structure is also found in IpTx$_a$ (Lee *et al.*, 2004)

and MCa (Mosbah *et al.*, 2000), as well as in ω-conotoxins (as discussed in Zhu *et al.*, 2003), highly potent blockers of voltage-gated Ca$^{2+}$ channels, suggesting that the RyR-targeting scorpion toxin-scaffold is a general molecular topology of exogenous toxins targeting Ca$^{2+}$ channels. Unlike IpTx$_a$ and MCa, which form the canonical anti-parallel β-sheets, HdCa's residues lack propensity to form β-sheets; however, it adopts the same globular structure because of the stability conferred by similar disulphide bridges. More importantly perhaps, and again unique to HdCa, is the fact that its basic residues appear to be spirally oriented along the long axis of the molecule, as opposed to the preferential segregation of these residues in MCa and IpTx$_a$, where they impart a high degree of amphipathicity. The relatively uniform distribution of positive charges in HdCa, due to the reshuffling and extra amount of basic residues, effectively reduces the dipole moment of the molecule and produces a globular peptide with little amphipathicity, which runs counter to the notion that amphipathicity is required for calcins to penetrate cellular membranes (Estève *et al.*, 2005; Mabrouk *et al.*, 2007). We thus favour the notion that a specific arrangement of basic residues plus the ICK motif determines, to a great extent, whether certain peptides penetrate the hydrophophic environment within cellular membranes. In favour of this notion, the trypsin inhibitors MCoTI-II and McoEeTI, peptides apparently unrelated to calcins but folding along an ICK motif and bearing the sequence KKCXR (present in all calcins), efficiently penetrate cellular membranes (Craik *et al.*, 2006). But proposing a signature sequence for cell-penetrating peptides has not worked well in the past (Kerkis *et al.*, 2006), and further experiments are needed to determine whether this apparently lax requirement holds true for natural or artificial variants of the present family of calcins. Challenging this notion, for example, is the recent study showing that *linearized* (disulphide-less) analogues of MCa retain the ability to translocate across cell membranes (Ram *et al.*, 2008), albeit at very high concentrations (10–100 µmol·L$^{-1}$).

*Single channel effects*

A characteristic effect of calcins, including the presently characterized HdCa, is the induction of a long-lived, reversible and barely fluctuating subconductance state in single channel recordings of RyRs (Zamudio *et al.*, 1997; Trypathy *et al.*, 1998; Gurrola *et al.*, 1999; Faljoun *et al.*, 2000; Shahbazzadeh *et al.*, 2007). This calcin-induced gating behaviour is similar in several features to the classical effect of ryanodine (Rousseau *et al.*, 1987), with the notable exception that the alkaloid is recalcitrant to dissociation and 'locks' the channel in a subconductance state that is irreversible during the time course of a bilayer experiment. By contrast, the four calcins so far tested for single channel effects exhibit 'on and off' mechanisms that allow for rapid binding to, and dissociation from, the channel. However, even within this defined scheme of interaction with the channel, subtle differences between calcins may be noted: the subconductance state that HdCa induces on RyR1 represents ~35% of the full opening (Figure 6), compared with 25–30% by IpTx$_a$ (Trypathy *et al.*, 1998; Gurrola *et al.*, 1999), ~50% by MCa (Faljoun *et al.*, 2000) and 38% by HCa (Shahbazzadeh *et al.*, 2007). Although the underlying

mechanism and precise peptide domain involved in this effect have yet to be identified, these differences probably arise from the structural diversity of calcins. However, the fact that the same peptide (HdCa) induced subconductance states of different amplitude in each RyR isoform (35% in RyR1 and 50% in RyR2, Figures 6 & 7 respectively) indicates that the interacting site of the channel is also structurally different. The apparent lack of effect of MCa on RyR2 (Altafaj *et al.*, 2007), contrasted with its robust effect on RyR1, also indicates that the binding domain is structurally diverse. The identification of the precise amino acid sequence of RyR1 and RyR2 that interacts with these peptides will clearly aid in the elucidation of the structural mechanism involved in the formation of the calcin–RyR high affinity complex.

*Cell-permeating properties of HdCa*

The membrane-permeating capacity of MCa has been investigated at several levels, but the time course of penetration of a calcin member has not been approached as precisely as in this study. The use of cardiac ventricular myocytes, with robust expression of RyRs and highly coordinated $Ca^{2+}$ release, provided a valid system to test the kinetics of penetration of unmodified (native) HdCa, free of cargo or fluorescent derivatives that could hinder its transit through cellular membranes. As cardiomyocytes are bathed in a solution containing $10^4$-fold more $Ca^{2+}$ outside than inside of the cell (1 mmol·$L^{-1}$ vs. ~0.1 µmol·$L^{-1}$ [$Ca^{2+}$]), any compromised membrane permeability is readily noticed by an uncontrolled influx of $Ca^{2+}$ followed by sustained contracture and cell death. Thus, only intact cardiomyocytes respond to field stimulation with coordinated $Ca^{2+}$ release or, if non-stimulated, maintain energy-driven $Ca^{2+}$ extrusion mechanisms that avoid $Ca^{2+}$ overflow. Under these conditions, rapid (≤50 ms) perfusion of HdCa onto the surface of *intact* cardiomyocytes produced two discernable effects: on paced cells, HdCa dramatically modified the amplitude of the [$Ca^{2+}$]$_i$ transient, initially increasing its amplitude and later producing a lower steady state with spontaneous $Ca^{2+}$ release. The initial effect had a rapid onset (~2 s) and was our best indicator that the peptide penetrates the external membrane of cardiomyocytes with remarkably rapid kinetics. The brevity of the increase in amplitude, combined with the lack of effect on time course of the $Ca^{2+}$ transient, may seem counterintuitive in light of the long subconducting states induced by HdCa in single channel experiments. Sobie *et al.* (2006) have suggested that leak from the SR may occur through a mechanism that is largely invisible by means of confocal microscopy. This may be true of the subconducting states, which may be masked by the initial, dramatic increase in transient amplitude.

In quiescent cells, HdCa induced the release of $Ca^{2+}$ from internal stores, also with remarkable speed (lag time ~2 s). This effect may seem contradictory to the results of [$^3$H]ryanodine binding assays, in which the toxin had no effect at $Ca^{2+}$ concentrations approximating those found in the resting cell. However, it is well documented that stochastic $Ca^{2+}$ release events occur in the cellular milieu (Cheng *et al.*, 1993), which are visualized as $Ca^{2+}$ sparks when a cluster of RyRs fires together. We believe that binding of HdCa to these open RyRs would be sufficient to simultaneously activate numerous clus-

ters of RyR and trigger a coordinated release of SR $Ca^{2+}$ stores. The amplitude of $Ca^{2+}$ release is similar to caffeine-induced $Ca^{2+}$ release events, but the effect of HdCa was consistently of shorter duration than that of caffeine, perhaps reflecting a faster dissociation from RyRs than seen with caffeine. However, low caffeine concentrations produce a $Ca^{2+}$ transient profile in which a sharp increase in amplitude is followed by a decrease to a steady state at diminished amplitude (Trafford *et al.*, 2000), an effect strikingly similar to that induced by HdCa and attributed to depleted SR $Ca^{2+}$ content. Both HdCa and caffeine bind to RyRs and induce $Ca^{2+}$ release, but they appear to bind to different sites and exert their effects through different mechanisms of action, as deduced from results such as those shown in Figure 4, where HdCa and caffeine have a synergistic interaction with the RyR by binding to two separate but apparently interacting sites. It is therefore expected that both of these agonists produce somewhat different macroscopic events in cellular experiments. However, elucidation of the detailed mechanism of action of HdCa requires further investigation.

In summary, we have purified, sequenced, structurally modelled and functionally characterized a novel member of the calcin family that expands our understanding of the structure–function relationship of this group of scorpion peptides. Several structural and functional attributes make HdCa unique among calcins: (i) it is the first 35-mer peptide (instead of the common 33-mer arrangement); (ii) it contains 14 (instead of 13) basic residues, uniformly distributed and spirally arranged; (iii) it does not exhibit prominent amphipathicity, yet it penetrates cellular membranes, challenging the notion that amphipathicity is required for calcins to penetrate cells; and (iv) it permeates ventricular cardiomyocytes and modifies $Ca^{2+}$ release, suggesting rapid penetration and binding to RyRs to produce derangement of coordinated $Ca^{2+}$ release. All of these attributes are likely to contribute to the capacity of scorpion venom to immobilize its prey.

## Acknowledgements

## Conflict of interest

None.

## References

Altafaj X, France J, Almassy J, Jona I, Rossi D, Sorrentino V *et al.* (2007). Maurocalcine interacts with the cardiac ryanodine receptor without inducing channel modification. *Biochem J* **406**: 309–315.

Berridge MJ (1997). The AM and FM of calcium signaling. *J Physiol* **499**: 291–306.

Bers DM (2001). *Excitation-Contraction Coupling & Cardiac Contractile Force*, 2nd edn. Kluwer Academic Publishers: Amsterdam.

Boisseau S, Mabrouk K, Ram N, Garmy N, Collin V, Tadmouri A *et al.* (2006). Cell penetration properties of maurocalcine, a natural venom peptide active on the intracellular ryanodine receptor. *Biochim Biophys Acta* **1758**: 308–319.

Cheng H, Lederer WJ, Cannell MB (1993). Calcium sparks: elementary events underlying excitation-contraction coupling in heart muscle. *Science* **262**: 740–744.

Craik DJ, Cemazar M, Wang CK, Daly NL (2006). The cyclotide family of circular miniproteins: nature's combinatorial template. *Biopolymers* **84**: 250–266.

El-Hayek R, Lokuta AJ, Arévalo C, Valdivia HH (1995). Peptide probe of ryanodine receptor function. *J Biol Chem* **270**: 28696–28704.

Estève E, Mabrouk K, Dupuis A, Smida-Rezgui S, Altafaj X, Grunwald D *et al.* (2005). Transduction of the scorpion toxin maurocalcine into cells: evidence that the toxin crosses the plasma membrane. *J Biol Chem* **280**: 12833–12839.

Faljoun Z, Kharrat R, Chen L, Lecomte C, Di Luccio E, Bichet D *et al.* (2000). Chemical synthesis and characterization of maurocalcine, a scorpion toxin that activates Ca(2+) release channel/ryanodine receptors. *FEBS Lett* **469**: 179–185.

Fill M, Copello JA (2002). Ryanodine receptor calcium release channels. *Physiol Rev* **82**: 893–922.

Gurrola GB, Arévalo C, Sreekuma R, Lokuta AJ, Walker JW, Valdivia HH (1999). Activation of ryanodine receptors by imperatoxin A and a peptide segment of the II-III loop of the dihydropyridine receptor. *J Biol Chem* **274**: 7879–7886.

Kerkis A, Hayashi MAF, Yamane T, Kerkis I (2006). Properties of cell penetrating peptides (CPPs). *IUBMB Life* **58**: 7–13.

Lai FA, Erickson HP, Rousseau E, Liu QY, Meissner G (1988). Purification and reconstitution of the calcium release channel from skeletal muscle. *Nature* **331**: 315–319.

Lee CW, Lee EH, Takeuchi K, Takahashi H, Shimada I, Sato K *et al.* (2004). Molecular basis of the high-affinity activation of type 1 ryanodine receptors by imperatoxin A. *Biochem J* **377**: 385–394.

Li P, Chen SRW (2001). Molecular basis of Ca$^{2+}$ activation of the mouse cardiac Ca$^{2+}$ release channel (ryanodine receptor). *J Gen Physiol* **118**: 33–44.

Liu Z, Zhang J, Li P, Chen SRW, Wagenknecht T (2002). Three-dimensional reconstruction of the recombinant type 2 ryanodine receptor and localization of its divergent region 1. *J Bio Chem* **277**: 46712–46719.

Mabrouk K, Ram N, Boisseau S, Strappazzon F, Rehaim A, Sadoul R *et al.* (2007). Critical amino acid residues of maurocalcine involved in pharmacology, lipid interaction and cell penetration. *Biochim Biophys Acta* **1768**: 2528–2540.

Meissner G, Henderson JS (1987). Rapid calcium release from cardiac sarcoplasmic reticulum vesicles is dependent on Ca$^{2+}$ and is modulated by Mg$^{2+}$, adenine nucleotide, and calmodulin. *J Biol Chem* **262**: 3065–3073.

Mitra R, Morad M (1985). A uniform enzymatic method for dissociation of myocytes from hearts and stomachs of vertebrates. *J Physiol* **249**: H1056–H1060.

Mosbah A, Kharrat R, Fajloun Z, Renisio JG, Blanc E, Sabatier JM *et al.* (2000). A new fold in the scorpion toxin family, associated with an activity on a ryanodine-sensitive calcium channel. *Proteins* **40**: 436–442.

Narasimhan L, Singh J, Humblet C, Guruprasad K, Blundell T (1994). Oxidative folding intermediates with nonnative disulfide bridges between adjacent cysteine residues. *Nat Struct Biol* **1**: 850–852.

Pallaghy PK, Nielsen KJ, Craik DJ, Norton RS (1994). A common structural motif incorporating a cystine knot and a triple-stranded {beta}-sheet in toxic and inhibitory polypeptides. *Protein Sci* **3**: 1833–1839.

Possani LD, Becerril B, Delepierre M, Tytgat J (1999). Scorpion toxins specific for Na$^+$ channels. *Eur J Biochem* **264**: 287–300.

Ram N, Weiss N, Texier-Nogues I, Aroui S, Andreotti N, Pirollet F *et al.* (2008). Design of a disulfide-less, pharmacologically-inert and chemically-competent analog of maurocalcine for the efficient transport of impermeant compounds into cells. *J Biol Chem* **283**: 27048–27056.

Rousseau E, Smith SJ, Meissner G (1987). Ryanodine modifies conductance and gating behavior of single Ca$^{2+}$ release channel. *J Physiol* **253**: C364–C368.

Rousseau E, Ladine J, Liu QY, Meissner G (1988). Activation of the Ca$^{2+}$ release channel of skeletal muscle sarcoplasmic reticulum by caffeine and related compounds. *Arch Biochem Biophys* **267**: 75–86.

Schwartz EF, Schwartz CA, Gómez-Lagunas F, Zamudio FZ, Possani LD (2006). HgeTx1, the first K(+)-channel specific toxin characterized from the venom of the scorpion *Hadrurus gertschi* Soleglad. *Toxicon* **48**: 1046–1053.

Shahbazzadeh D, Srairi-abid N, Feng W, Ram N, Borchani L, Ronjat M *et al.* (2007). Hemicalcin, a new toxin from the Iranian scorpion *Hemiscorpius lepturus* which is active on ryanodine-sensitive Ca$^{2+}$ channels. *Biochem J* **404**: 89–96.

Sobie EA, Guatimosim S, Gómez-Viques L, Song L, Harmann H, Jafri MS *et al.* (2006). The Ca$^{2+}$ leak paradox and 'rogue ryanodine receptors': SR Ca$^{2+}$ efflux theory and practice. *Prog Biophys Mol Biol* **90**: 172–185.

Sutko JL, Airey JA, Welch W, Ruest L (1997). The pharmacology of ryanodine and related compounds. *Pharmacol Rev* **49**: 53–98.

Trafford AW, Sibbring GC, Díaz ME, Eisner DA (2000). The effects of low concentrations of caffeine on spontaneous Ca release in isolated rat ventricular myocytes. *Cell Calcium* **28** (4): 269–276.

Trypathy A, Resch W, Xu L, Valdivia HH, Meissner G (1998). Imperatoxin A induces subconductance states in Ca$^{2+}$ release channels (ryanodine receptors) of cardiac and skeletal muscle. *J Gen Physiol* **111**: 679–690.

Valdivia HH, Kirby MS, Lederer WJ, Coronado R (1992). Scorpion toxins targeted against the sarcoplasmic reticulum Ca(2+)-release channel of skeletal and cardiac muscle. *Proc Natl Acad Sci USA* **89**: 12185–12189.

Zamudio FZ, Gurrola GB, Arevalo C, Sreekumar R, Walker JW, Valdivia HH *et al.* (1997). Primary structure and synthesis of Imperatoxin A (IpTxa), a peptide activator of Ca$^{2+}$ release channels/ryanodine receptors. *FEBS Lett* **405**: 385–389.

Zhu S, Darbon H, Dyason K, Verdonck F, Tytgat J (2003). Evolutionary origin of inhibitor cystine knot peptides. *FASEB J* **17**: 1765–1767.

## Supporting Information

Additional Supporting Information may be found in the online version of this article:

Accelrys Discovery Studio PDB file

Please note: Wiley-Blackwell are not responsible for the content or functionality of any supporting materials supplied by the authors. Any queries (other than missing material) should be directed to the corresponding author for the article.